



Original

miR-374 improves cerebral ischemia reperfusion injury by targeting *Wnt5a*

Fangyuan XING¹⁾, Yongrong LIU²⁾, Ruifang DONG¹⁾ and Ye CHENG¹⁾¹⁾Department of Neurology, Cangzhou Central Hospital, No. 16 Xinhua West Road, Cangzhou, Hebei 061000, People's Republic of China²⁾Department of Ultrasound, Cangzhou Central Hospital, No. 16 Xinhua West Road, Cangzhou, Hebei 061000, People's Republic of China

Abstract: To date, studies have demonstrated the potential functions of microRNAs in cerebral ischemia reperfusion (IR) injury. Herein, we established a middle cerebral artery occlusion (MCAO) model in rats and then subjected them to reperfusion to explore the role of microRNA-374 (miR-374) in cerebral IR injury. After reperfusion, the endogenous miR-374 level decreased, and the expression of its target gene, *Wnt5a*, increased in brain tissues. Intracerebral pretreatment of miR-374 agomir attenuated cerebral damage induced by IR, including neurobehavioral deficits, infarction, cerebral edema and blood-brain barrier disruption. Moreover, rats pretreated with miR-374 agomir showed a remarkable decrease in apoptotic neurons, which was further confirmed by reduced BAX expression as well as increased BCL-2 and BCL-XL expression. A dual-luciferase reporter assay substantiated that *Wnt5a* was the target gene of miR-374. miR-374 might protect against brain injury by downregulating *Wnt5a* in rats after IR. Thus, our study provided a novel mechanism of cerebral IR injury from the perspective of miRNA regulation.

Key words: brain ischemia, miR-374, reperfusion injury, *Wnt5a*

Introduction

Ischemic stroke, also known as ischemic cerebrovascular disease (ICVD) and cerebral infarction, is a kind of disease involving brain tissue necrosis that caused by stenosis or occlusion of a cerebral blood supply artery and insufficient blood supply to the brain. Ischemic stroke is one of the leading causes of mortality and serious long-term disability, making it the most common life-threatening neurological disease [1]. About 15 million patients suffer an ischemic stroke each year globally, resulting in death in over 5 million of the patients and permanent disability in another 5 million [2]. Moreover, the incidence of recurrent ischemic stroke is 11.3% after 5 years [3]. Problems such as motor dysfunction after an ischemic stroke and recurrence seriously affected the quality of life of patients. Although restoration

of the blood supply through reperfusion can improve clinical outcomes, rapid reperfusion may also result in the exacerbation of cerebral injury [4]. Cerebral ischemia reperfusion (IR) injury has become an increasingly tough challenge for stroke patients. Therefore, efforts to further study effective prevention and management in ischemic stroke are urgently needed.

MicroRNAs (miRNAs) are a class of small non-coding RNAs that play important roles in cerebral IR injury by regulating the expression of target genes [5, 6]. For example, miR-106b-5p ameliorates cerebral IR injury by inhibiting apoptosis and oxidative stress [7]. miR-431 exerts protective effects against cerebral IR injury by targeting the Rho/Rho-kinase signaling pathway [8]. Recent evidence suggests that supplementation with miR-7 mimics may be a therapeutic option to minimize stroke-induced brain damage and disability [9]. miR-374

(Received 2 April 2020 / Accepted 24 September 2020 / Published online in J-STAGE 27 October 2020)

Corresponding author: F. Xing. e-mail: xfy01020304@163.com



This is an open-access article distributed under the terms of the Creative Commons Attribution Non-Commercial No Derivatives (by-nc-nd) License <<http://creativecommons.org/licenses/by-nc-nd/4.0/>>.

©2021 Japanese Association for Laboratory Animal Science

was previously found to display an increasing expression level in an embolic stroke model [10] and was later discovered to protect against myocardial IR injury in adult rodents. Zhang *et al.* demonstrated that miR-374 mitigated rat myocardial IR injury by targeting SP1 through the activation of the PI3K/Akt signal pathway after pretreatment with sevoflurane [11]. Another study conducted by Zhao *et al.* showed that miR-374 alleviated myocardial IR injury in mice after thoracic epidural anesthesia by suppressing the activity of a DTNA-mediated Notch1 axis [12]. The above studies revealed that miR-374 might be a therapeutic target for IR injury, but all of them focused on the myocardium; its effect on cerebral IR injury is far from being elucidated, and the underlying mechanism also needs to be further studied.

Wnt5a is a signaling molecule belonging to the large Wnt family. As an extracellular ligand of the Wnt non-canonical pathway, it regulates the β -catenin-independent pathway by binding to plasma membrane receptors or co-receptor complexes and activating Dishevelled (Dvl) phosphoproteins in the cytoplasm [13], which modulates various cellular functions, including migration, adhesion, invasion, metastasis, and differentiation [14–17]. It is well known that abnormalities of Wnt5a signaling are involved in several human diseases, such as cancers, inflammatory diseases, and metabolic disorders [18–21]. Previous evidence suggested that noncanonical Wnt5a/JNK signaling was implicated in cardiac injury under ischemic stress, and this signaling was suppressed by Sfrp5, thereby protecting the heart from IR injury [22]. Furthermore, Wnt5a has been reported to play a crucial role in stroke. Both *in vitro* and *in vivo* studies have shown that inhibition of Wnt5a could alleviate cerebral IR injury, which provided a novel target for stroke therapy [23].

Given that *Wnt5a* is a target gene of miR-374 (predicted with TargetScan and the Starbase database), we hypothesized that miR-374 may regulate cerebral IR injury through targeting of *Wnt5a*. Therefore, our study investigated the role of miR-374 in brain IR injury and neuronal apoptosis in a rat model of cerebral IR and whether it was associated with its targeting of *Wnt5a*.

Materials and Methods

Animals and grouping

Adult male Sprague-Dawley rats (weighing 230–250 g) were purchased from Changsheng Biotechnology (Liaoning, China) and maintained under optimal conditions (25 ± 1°C, 45–55% humidity, and a 12 h light/dark cycle). All animal experiments were approved by the animal research ethics committee of Cangzhou Central

Hospital and performed in accordance with the Guide for Laboratory Animal Care and Use. The animal experiment consisted of three parts. For the first part, the rats were randomly assigned to two groups, with 6 rats in each group: the sham and IR groups. For the second part, the rats were randomly assigned to five groups, with 6 rats in each group: the control, sham 6 h, IR 6 h, IR 24 h, and IR 72 h groups. For the third part, the rats were randomly assigned to four groups, with 36 rats in each group: the sham, IR, IR + NC agomir, IR 24 h + miR-374 agomir groups. After the experiment, the rats were sacrificed by CO₂ inhalation. The rats from each group were then randomly assigned for different determinations: six rats in each group were used for the determination of neurobehavioral score, six rats in each group were used for the evaluation of infarct volume, six rats in each group were used for real-time PCR and Western blot analyses, six rats in each group were used for the evaluation of brain water content, six rats in each group were used for the measurement of blood-brain barrier leakage by Evans, and six rats in each group were used for immunofluorescence staining.

Establishment of rat models of cerebral IR injury

Anesthesia was induced with 1% pentobarbital (40 mg/kg, i.p.). After midline neck incision, the right common carotid artery (CCA), internal carotid artery (ICA), and external carotid artery (ECA) were exposed and isolated. The CCA and ECA were then ligated with 3–0 monofilament respectively. A polylysine-coated nylon filament was employed as an embolus and inserted into the ICA through the ECA stump to occlude the middle cerebral artery. The filament was pushed through the carotid bifurcation and 18–22 mm into the ICA, stopping when there was slight resistance. After 120 min of ischemia, the rat models of middle cerebral artery occlusion (MCAO) was established, and the nylon filament was then withdrawn for 24 h of reperfusion. In the sham procedure, rats were treated identically without occlusion of the middle cerebral artery.

Intracerebroventricular pretreatment

Rats were injected intracerebrally 2 h before MCAO. They were anesthetized with pentobarbital and placed in a stereotaxic frame. A puncture needle was implanted stereotaxically into the infarct side ventricle (bregma, posterior 0.8 mm; median line, right 1.5 mm; bone surface, downwards 4.5 mm). miR-374 agomir or negative control agomir (3 pmol/g body weight in 2 μ l) was mixed with cationic lipid DOTAP (4 μ l, 6 μ l total volume) and was injected via microinfusion pump (0.5 μ l/min). Agomir is a specially labeled and chemically modified

double-stranded small RNA that mimics the endogenous miRNA to regulate the biological function of target genes. The sequences of miR-374 agomir and NC agomir are as follows: 5'-AUAUAAUACAACCUGCU-AAGUG-3' (sense) and 5'-CUUAGCAGGUUGUAU-UUAUUU-3' (antisense) for miR-374 agomir and 5'-UUCUCCGAACGUGUCACGUTT-3' (sense) and 5'-ACGUGACACGUUCGGAGAATT-3' (antisense) for NC agomir.

Neurobehavioral score

The neurobehavioral scores of rats were determined after 24 h of reperfusion. The scoring system was composed with motor tests, sensory tests, beam balance tests, and tests for reflex absence and abnormal movements. Neurological function was scored on a scale of 0 to 18 (0, normal score; 18, maximal deficit score). The procedures performed in the above tests were described in a previous study [24]. In injury severity scoring, one point is awarded for inability to perform a task or for the lack of a tested reflex; the higher the score, the more serious the injury.

Infarct volume

After sacrifice, brains were removed, frozen at -20°C for 30 min to fix the brain tissues, and cut into 2 mm slices. Slices were incubated in 1% 2,3,5-triphenyltetrazolium chloride (TTC) for 15 min at 37°C . Images of brain sections were recorded. The infarct volume was calculated using the ImageJ software and was determined by infarction rate (%) = the infarct volume / the volume of the homolateral hemisphere $\times 100$.

Real-time PCR

An RNAsimple Total RNA Kit (DP419, Tiangen Biotech, Beijing, China) was used to extract total RNA from brain tissues. Briefly, tissues were added with 1 ml Buffer RZ and homogenized. The homogenized samples were incubated at room temperature for 5 min. After centrifuging at 10,000 g for 10 min at 4°C , the colorless upper aqueous phase (containing RNA) was pipetted into a new tube. Then 0.5 volumes of ethanol was added to the aqueous phase and mixed thoroughly. The sample was transferred to an RNase-Free spin column CR3 placed in an RNase-Free collection tube. After centrifuging at 10,000 g for 30 s at 4°C , the flow-through was discarded. Then, Buffer RD (500 μl) was added to the spin column CR3. After centrifuging at 10,000 g for 30 s at 4°C , the flow-through was discarded, and then 500 μl Buffer RW was added to the spin column CR3. After incubating at room temperature for 2 min and centrifuging at 10,000 g for 30 s at 4°C , the flow-through was discarded; this step was

repeated after adding 500 μl Buffer RW to the spin column CR3. The spin column CR3 was set back in the collection tube and centrifuged at 10,000 g for 2 min at 4°C . It was then placed in a new RNase-Free collection tube. After adding 30–100 μl RNase-Free ddH₂O, the column was incubated at room temperature for 2 min. RNA was eluted after centrifugation at 10,000 g or 2 min at 4°C , and the concentration was determined. RNA was reverse transcribed with M-MLV Reverse Transcriptase (NG212, Tiangen Biotech). Real-time PCR reactions were conducted with SYBR Green (SY1020, Solarbio, Beijing, China) and 2 \times Taq PCR MasterMix (KT201, Tiangen Biotech). The primers used were as follows: 5'-ACAGCCGCTTCAACTCCCCAACC-3', forward, and 5'-TCGCAGCCGTCCATCCCCTCT-3', reverse, for *Wnt5a*; 5'-CGGCAAGTTCAACGGCACAG-3', forward, and 5'-CGCCAGTAGACTCCACGACAT-3', reverse, for *Gapdh*; 5'-GTTGGCTCTGGTGCAGGGTC-CGAGGTATTCGCACCAGAGCCAACCACTTA-3', RT primer, 5'-ATATAATACAACCTGCTAAGTG-3', forward, and 5'-GCAGGGTCCGAGGTATTC-3', reverse, for rno-miR-374-5p; and 5'-GTTGGCTCTGGTGCAGGGTCCGAGGTATTCGCACCAGAGCCAA-C A A G C C T A C - 3', RT primer, 5'-GATCTCGGAAGCTAAGCAGG-3', forward, and 5'-TGGTGCAGGGTCCGAGGTAT-3' reverse, for 5s. Measurements for mRNA were normalized to *Gapdh*, and rno-miR-374-5p was normalized to 5s. The relative expression was obtained using the $2^{-\Delta\Delta\text{Ct}}$ method.

Western blot analysis

Brain tissues were collected and lysed with RIPA lysis buffer (R0010, Solarbio) plus phenylmethylsulfonyl fluoride (P0100, Solarbio). A BCA Protein Assay Kit (PC0020, Solarbio) was used to measure protein concentrations. After separation with 8–15% sodium dodecyl sulfate-polyacrylamide gel, the proteins were transferred to PVDF membranes. Then the membranes were blocked with 5% non-fat milk and incubated with primary antibodies and corresponding secondary antibodies (Solarbio). The protein bands were visualized with an enhanced chemiluminescence reagent (PE0010, Solarbio). The primary antibodies were as follows: Wnt5a antibody (DF6856, Affinity, Cincinnati, OH, USA), Bcl-x1 antibody (AF6414, Affinity), Bcl-2 antibody (AF6139, Affinity), Bax antibody (AF0120, Affinity), GAPDH antibody (60004-1-Ig, Proteintech, Wuhan, China).

Measurement of brain water content

After 24 h of reperfusion, rats were sacrificed, and their brains were removed. The fresh brain tissues from

the ischemic hemisphere were weighed to obtain the wet weight and then dried in an oven at 100°C for 24 h to obtain the dry weight. The brain water content (%) was calculated as follows: (wet weight – dry weight) / wet weight × 100.

Evans blue injection and brain extraction

The blood-brain barrier (BBB) leakage was measured by Evans blue (EB) staining as described previously [25]. Briefly, rats were subjected to tail vein injection with 2% Evans blue (2 ml/kg), and sacrificed 1 h after the injection. After thoracotomy, perfusion with normal saline through the left ventricle was performed to wash away any remaining dye within the blood vessels. The ischemic hemisphere was removed and weighed to determine the wet weight. Evans blue was extracted by adding 1 ml formamide to 100 mg of tissue, followed by incubation at 37°C for 24 h. The extracted Evans blue was centrifuged, and the supernatant was collected and subjected to measurement of absorbance at 632 nm. Evans blue solutions with different concentrations was generated and measured at 632 nm to produce a standardized curve. The amount of Evans Blue (μg) extravasated per g tissue was then calculated based on the standardized curve.

TUNEL-NeuN double immunofluorescence staining

After 24 h of reperfusion, rats were sacrificed, and their brains were collected. The brains were fixed in 10% formalin, embedded in paraffin, and cut into 5 μm slices. After paraffin removal with xylene and rehydration with ethanol, the slices were permeabilized with 0.1% Triton X-100 (ST795, Beyotime, Shanghai, China). Antigen retrieval was performed using citric acid-sodium citrate solution. The sections were treated with 50 μl TUNEL solution (11684817910, Roche Molecular Biochemicals, Mannheim, Germany; enzyme solution: label solution = 1:9). Next, they were blocked with goat serum and then incubated with a primary antibody against NeuN (ab104224, Abcam, Cambridge, UK; 1:300), followed by incubation with a FITC-labeled goat anti-mouse IgG antibody (A0568, Beyotime; 1:200). The nuclei were stained with DAPI (C1002, Beyotime). After sealing with anti-fade reagent, the slices were observed using a fluorescent microscope ($\times 400$).

Double immunofluorescence staining

Sections were heated at 60°C for 2 h and then dewaxed and rehydrated. They were then treated with antigen retrieval solution and blocked with goat serum. Primary antibodies against Wnt5a (55184-1-AP, Proteintech; rabbit, 1:200) and NeuN (ab104224, Abcam; mouse, 1:300;

combined and diluted with PBS) were added to the sections, and the sections were then incubated overnight at 4°C. Subsequently, the sections were incubated with a Cy3-labeled goat anti-rabbit IgG antibody (A0516, Beyotime) or FITC-labeled goat anti-mouse IgG antibody (A0568, Beyotime; 1:200) for 90 min. The nuclei were stained with DAPI (C1002, Beyotime). The cells from each of the different brain tissue sections were visualized at 400 \times magnification with a microscope.

Analysis of luciferase activity

Wild-type *Wnt5a* 3'UTR was cloned downstream of the pmirGLO (E133A, Promega, Madison, WI, USA) vector. Mutations were performed in the binding sites. The pmirGLO vector plus miR-374 agomir or negative control agomir were transiently co-transfected into 293T cells (Zhong Qiao Xin Zhou Biotechnology, Shanghai, China). The activities of firefly and Renilla luciferases were measured with a dual-luciferase reporter assay kit (KeyGen Biotech, Nanjing, China).

Statistical analysis

Statistical analysis was performed with the unpaired *t*-test or one-way ANOVA followed by Dunnett's multiple comparisons or Tukey's multiple comparisons as post-hoc tests. Data are presented as the mean \pm SD deviation. $P < 0.05$ was considered statistically significant (* $P < 0.05$; ** $P < 0.01$; *** $P < 0.001$; **** $P < 0.0001$).

Results

Cerebral IR caused neurological deficit, cerebral infarct, downregulation of miR-374, and upregulation of Wnt5a

We first established a model of cerebral IR in male SD rats by reperfusion after MCAO. There were obvious differences in neurobehavioral deficits and infarct volume in the IR group compared with the sham group at 24 h after reperfusion (Figs. 1A–C). Next, effects of IR on the expression levels of miR-374 and Wnt5a were detected by real-time PCR and Western blot analysis (Figs. 1D and E). miR-374 expression progressively decreased from 6 h to 72 h after experimental cerebral IR in rats. On the other hand, the mRNA and protein expression levels of Wnt5a progressively increased in the IR group. These data demonstrated that cerebral IR altered the expression of miR-374 and Wnt5a in the rat brain.

Overexpression of miR-374 protected the brain from IR injury

We then investigated whether restoring the abundance

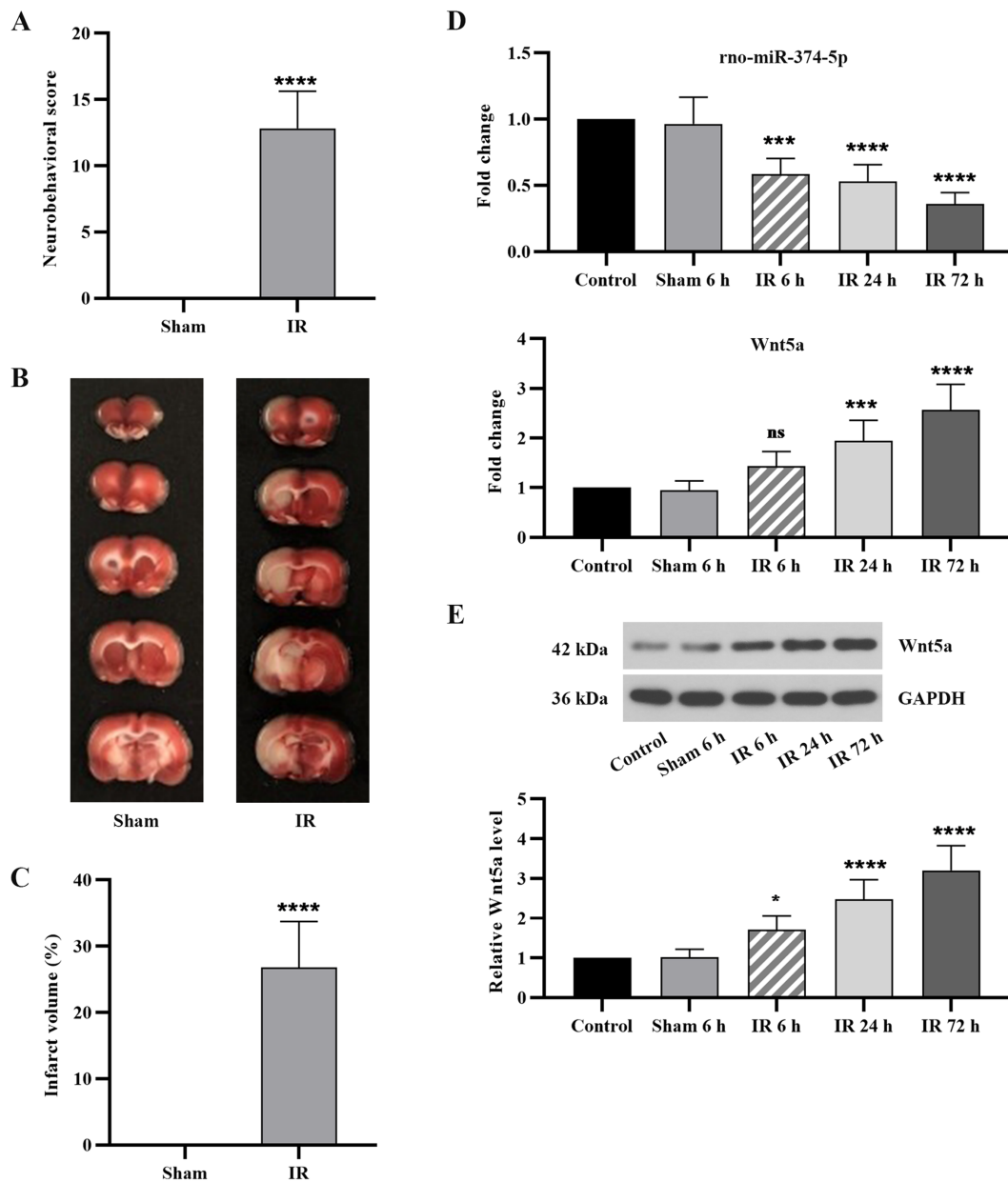


Fig. 1. Cerebral IR caused neurological deficit, cerebral infarct, downregulation of miR-374, and upregulation of Wnt5a. (A) The neurobehavioral scores of animals (evaluated 24 h after reperfusion). (B) Representative images of TTC-stained brain sections of rats (evaluated 24 h after reperfusion). (C) Quantification of infarct volume. (D) After 6 h, 24 h and 72 h of reperfusion, real-time PCR was performed to assess the abundance of miR-374 and *Wnt5a* in the brain tissues of rats. (E) After 6 h, 24 h and 72 h of reperfusion, the protein expression of WNT5A was determined by Western blot analysis. Data are presented as the mean \pm SD, and they were analyzed by unpaired t-test or one-way ANOVA followed by Dunnett's test. Compared with the sham group: * $P < 0.05$; *** $P < 0.001$; **** $P < 0.0001$.

of miR-374 by treating rats with miR-374 agomir improved brain injury after IR. miR-374 agomir was first injected intracerebrally 2 h before transient MCAO. After reperfusion for 24 h, real-time PCR was performed, and the result showed that miR-374 agomir effectively increased miR-374 expression, which indicated that transfection was successful (Fig. 2A). After pretreatment with miR-374 agomir, MCAO, and then reperfusion, neurobehavioral deficits were prominently improved

(Fig. 2B). The infarct volume measured at 24 h of reperfusion was smaller in the IR + miR-374 agomir group compared with the IR + NC agomir group (Figs. 2C and D). Similar results were observed when the brain water content was measured in the ischemic hemispheres (Fig. 2E). Moreover, the measurement of Evans blue extravasation was performed to evaluate the integrity of the BBB. The result data showed that cerebral IR caused disruption of the BBB but that it was rescued by pretreat-

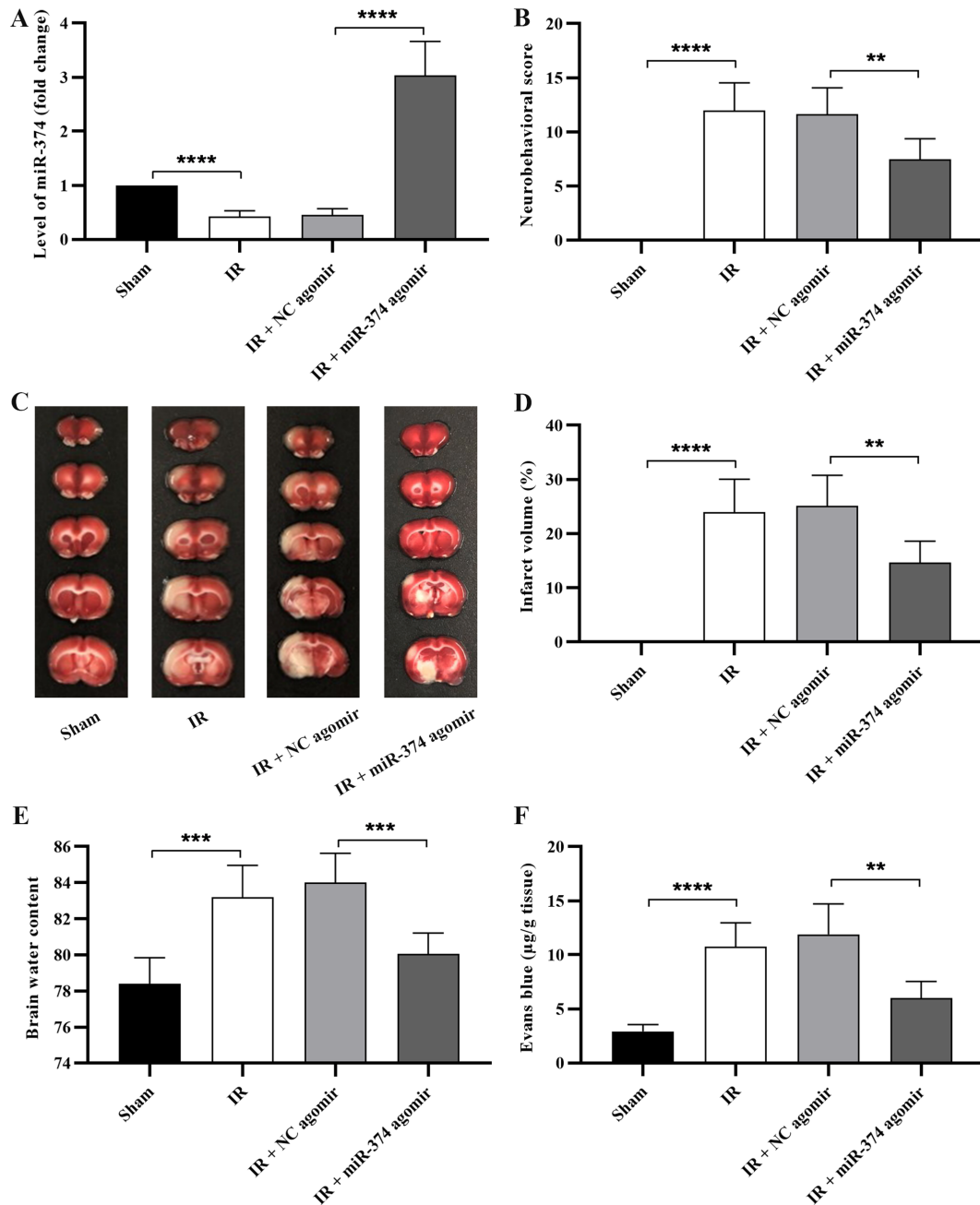


Fig. 2. Overexpression of miR-374 improved neurological deficit, cerebral infarct, cerebral edema, and disruption of the BBB after IR. (A) The levels of miR-374 in brain tissues of different groups. (B) Neurobehavioral scores of animals. (C) Representative images of TTC staining. (D) Quantification of infarct volume. (E) Quantification of the water content of the ischemic hemispheres. (F) Quantification of Evans Blue extravasation in the brain. Data are presented as the mean \pm SD, and they were analyzed by unpaired *t*-test. Comparison of the sham group with the IR group and the IR + NC agomir group with the IR + miR-374 agomir group: ** $P < 0.01$; *** $P < 0.001$; **** $P < 0.0001$.

ment with miR-374 agomir (Fig. 2F). Together, the above results implied that miR-374 provided protection against cerebral IR injury.

Overexpression of miR-374 attenuated cerebral IR-induced apoptosis

To identify neuron apoptosis in brain injury induced by IR, double immunofluorescence staining of TUNEL

and NeuN, a marker for neurons, was employed in brain tissue. TUNEL expression increased in neurons after cerebral IR. Pretreatment with miR-374 agomir reduced the number of TUNEL-positive neurons (Fig. 3A). In addition, the Western blot results showed increased expression of BAX and decreased expression of BCL-XL and BCL-2 in the IR group. However, the protein levels were reversed by pretreatment with miR-374 agomir

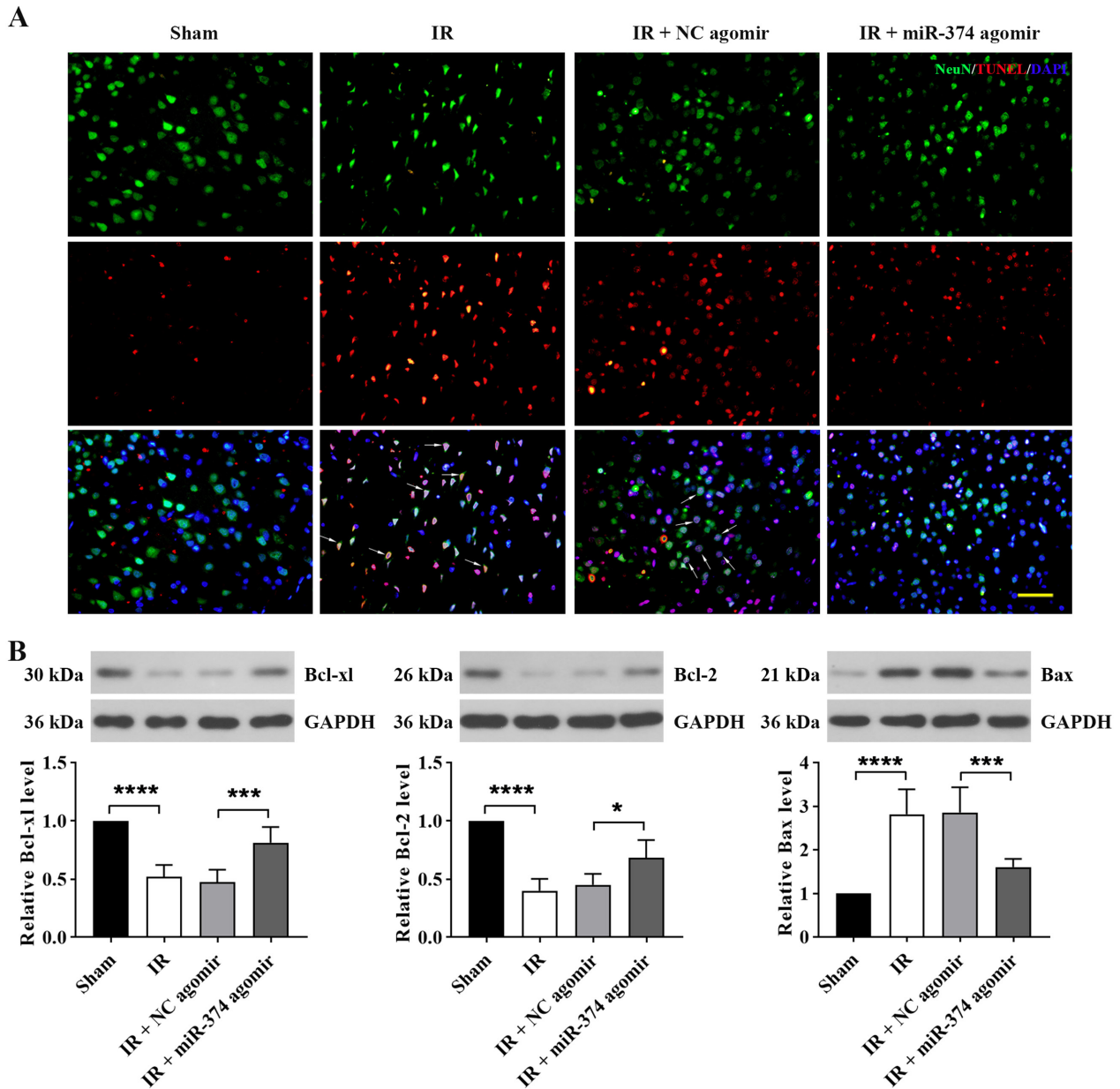


Fig. 3. Overexpression of miR-374 attenuated cerebral IR-induced apoptosis. (A) Immunostaining showing differences in neuronal apoptosis among groups. NeuN⁺/TUNEL⁺ colocalization is represented by arrows. Scale bar, 50 μ m. (B) Western blot showing expression of apoptosis-related proteins (BCL-XL, BCL-2, and BAX) in brain tissues. Data are presented as the mean \pm SD, and they were analyzed by unpaired *t*-test. Comparison of the sham group with the IR group and the IR + NC agomir group with the IR + miR-374 agomir group: * P <0.05; *** P <0.001; **** P <0.0001.

(Fig. 3B). These data suggested that miR-374 reduced neuron apoptosis after cerebral IR.

miR-374 directly targeted and suppressed *Wnt5a* expression in cerebral IR rats

Since TargetScan and the Starbase database showed the directly binding of miR-374 and *Wnt5a*, we first determined the level of *Wnt5a* after miR-374 agomir pretreatment and cerebral IR by real-time PCR and Western blot. As shown in Figs. 4A and B, pretreatment with miR-374 agomir markedly attenuated the increase in

Wnt5a level compared with the IR group. Double immunofluorescence confirmed the above results and further revealed the colocalization of *Wnt5a* with NeuN (Fig. 4C). Furthermore, the images also showed non-neuronal *Wnt5a*⁺ elements. Since previous studies demonstrated that *Wnt5a* is expressed in astrocytes in brain tissues of rodents [26, 27], we deduced that these elements might be astrocytes. A dual luciferase reporter assay was performed to validate the direct targeting of the *Wnt5a* 3'-UTR by miR-374. The relative luciferase activity of the *Wnt5a* wild-type 3'-UTR, but not the mu-

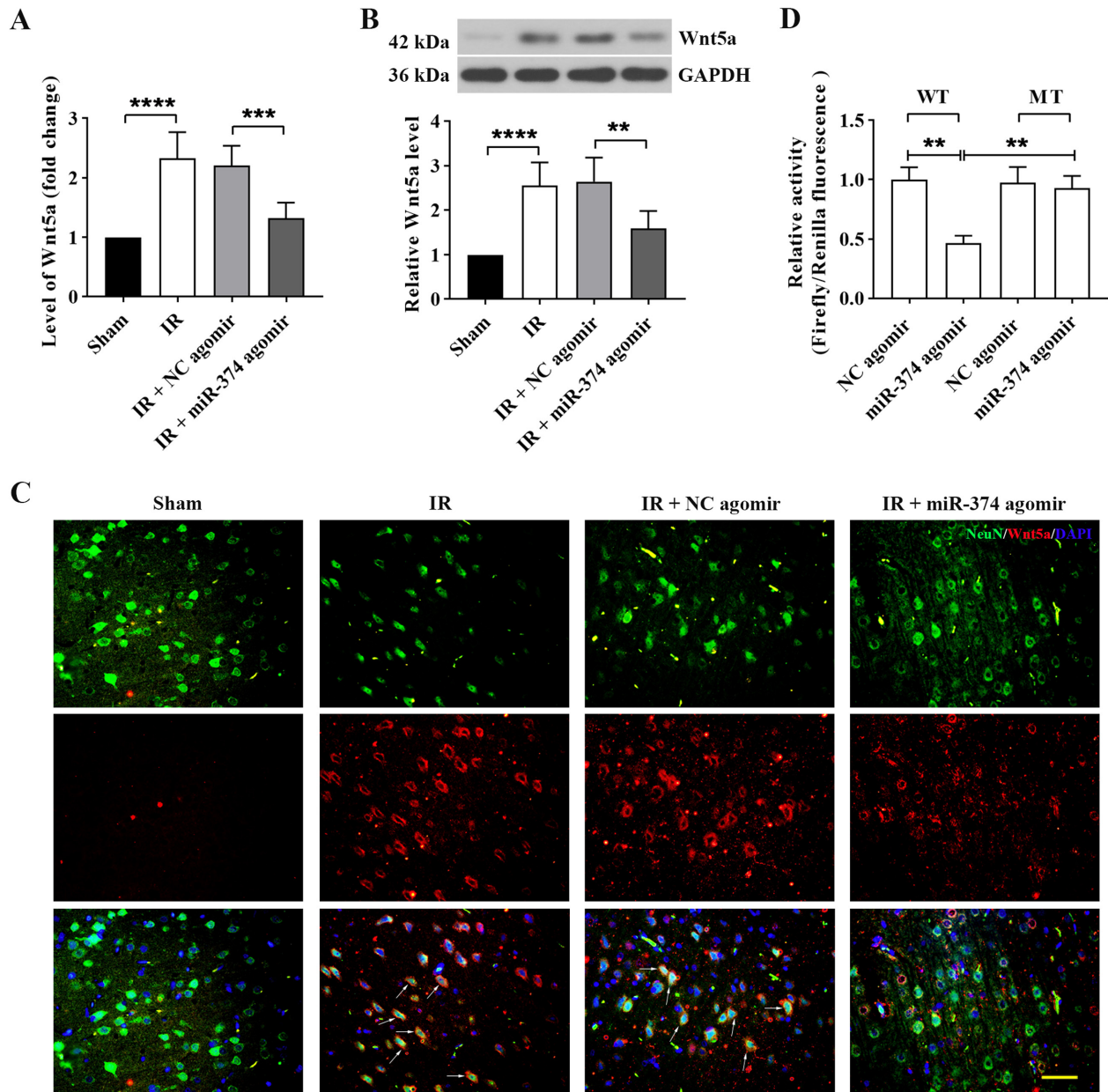


Fig. 4. miR-374 directly targeted and suppressed Wnt5a expression in cerebral IR rats. Rats were administrated with miR-374 agomir, and 24 h after cerebral IR, the expression of Wnt5a in brain tissues was analyzed with real-time PCR (A) and Western blot (B). (C) Representative immunofluorescence images showing colocalization of WNT5A in neurons. NeuN⁺/WNT5A⁺ colocalization is represented by arrows. Scale bar, 50 μ m. (D) The binding of miR-374 and Wnt5a was assessed using a dual-luciferase reporter assay in 293T cells. WT: wild type. MT: mutant type. Data in panels A, B, and D are shown as the mean \pm SD from three separate experiments, and comparisons were made with the unpaired *t*-test for A and B and with one-way ANOVA followed by Tukey's test as the post-hoc test for D.

tant 3'-UTR, was dramatically suppressed by miR-374 agomir (Fig. 4D). These results indicated that the effects of miR-374 in cerebral IR were associated with its targeting of Wnt5a.

Discussion

During focal cerebral ischemia, if blood flow cannot be restored to the ischemic penumbra or other measures

cannot be taken, the focal cerebral ischemia often develops into infarction that causes serious damage and may not be repairable. Reperfusion of the occluded vessels immediately is the gold standard for treatment of acute ischemic stroke [28]. Nevertheless, reperfusion may still further damage surrounding tissue by activating apoptosis and a neurodegenerative cascade [29]. At present, intravenous thrombolysis (rt-PA), neuronal repair therapy, and neuroprotective agents are the possible thera-

peutic options for ischemic stroke. However, the available treatments remain limited, and they have not yet achieved satisfactory efficacy and safety [30–32]. In the present research, we demonstrated that pretreatment with miR-374 agomir ameliorated brain injury induced by IR, as evidenced by a decreased brain infarct volume, decreased water content, improved neurobehavioral function and BBB disruption, and attenuated neuronal apoptosis. We also found that these effects of miR-374 were dependent on its targeting of Wnt5a. Our findings illuminated for the first time that miR-374 provides protection from cerebral IR injury, suggesting a possible clinical role for miR-374 in ischemic stroke treatment.

In the rat models of cerebral IR injury, we found that the expression of miR-374 significantly decreased, which was not in agreement with the finding of Liu *et al.* [10]. In their study, rats were subjected to MCAO only without reperfusion, and miR-374 showed a compensatory increase and exerted a protective effect after cerebral ischemia. In the rat model we established, reperfusion following MCAO may have exacerbated the deleterious effects caused by ischemia, thus leading to decreased miR-374 expression. Since miRNAs do not code for proteins, the protective effect of miR-374 on cerebral IR injury is assumed to be exerted via the regulation of its targets. A previous study showed that suppression of Wnt5a is neuroprotective after cerebral ischemia [23]. In the present study, in database predicted, we experimentally confirmed that *Wnt5a* transcripts are targets of miR-374, which was predicted by TargetScan and the Starbase database. Firstly, we observed a remarkable decrease in Wnt5a expression *in vivo* after inducing overexpression of miR-374 with agomir. Next, using the dual-luciferase assay, we substantiated the directly binding of miR-374 and Wnt5a. Overall, our study indicated that miR-374 mitigated post-ischemic brain damage by directly targeting to Wnt5a. Indeed, some other targets of miR-374 may also contribute to protection of the brain from IR injury, and future studies will assess their relevance to protection by knockdown of specific targets.

In the central nervous system (CNS), Wnt5a plays a crucial role in the postsynaptic region of central synapses. Wnt5a activates noncanonical Wnt signaling pathways, including Wnt/Ca²⁺ and Wnt/JNK signaling pathways, and then increases the clustering of PSD-95 and NMDAR [33, 34]. Furthermore, it regulates inhibitory synaptic transmission mediated by GABA_A receptors. As observed in hippocampal neurons, Wnt5a enhances the recycling of functional GABA_A receptors [33]. The above studies indicated that Wnt5a modulates the assembly and function of the excitatory postsynaptic

region of the brain. However, the role of Wnt5a in hippocampal neurons damaged by brain IR is far from being elucidated. In this study, we provided evidence for the role of Wnt5a in a rat model of cerebral IR. A limitation of the present study was that we did not investigate Wnt5a-mediated neuroprotection with intracellular experiments. Future work needs to be done to explore the protective effect of the miR-374/Wnt5a pathway on hippocampal neuronal cells subjected to oxygen glucose deprivation (OGD).

Apoptosis is a common process that occurs in brain damage caused by IR [35, 36]. The present study was undertaken to determine the effect of miR-374 on apoptosis. Our results showed miR-374 protected neurons from apoptosis, as evidenced by fewer TUNEL-positive cells in the brain tissue of the group pretreated with miR-374 agomir. The Bcl-2 family is a family of regulators comprised of anti- and pro-apoptotic members that arbitrate cellular life-or-death decisions. Bcl-2 and Bcl-xl, as anti-apoptotic members, prevent cells from undergoing apoptosis. By contrast, Bax is a positive regulator that initiates apoptosis. Both Bcl-2 and Bax regulate the release of cytochrome c or other apoptosis-inducing factors, and hence caspase cascade activation, which leads to apoptosis [37]. In this study, we found miR-374 up-regulated the expression of Bcl-xl and Bcl-2 and down-regulated Bax in brain tissues of cerebral IR rats. It has been proven that both apoptosis and autophagy are activated in the ischemic penumbra [38], and a transition from apoptosis to autophagy might occur in the subacute phase of stroke [39]. More broadly, the effect of miR-374 on autophagy in cerebral IR injury could be assessed in future research, which may yield further insight into the neuroprotective role of miR-374.

In conclusion, our study demonstrated that miR-374 improved brain injury and prevented neuronal apoptosis in cerebral IR rats. Furthermore, miR-374 played a protective role in cerebral IR injury by targeting Wnt5a. Taken together, identification of the miR-374/Wnt5a axis may provide new insight into the potential molecular mechanisms of cerebral IR injury.

Conflicts of Interests

The authors declare that they have no competing interests.

Authors' Contributions

Fangyuan Xing conceived the study. Fangyuan Xing and Yongrong Liu carried out the experiments. Ruifang Dong analyzed the data. Ye Cheng drafted the manu-

script. Fangyuan Xing revised the manuscript. All authors approved the final version of the manuscript.

Acknowledgements

Not applicable.

References

- Benjamin EJ, Muntner P, Alonso A, Bittencourt MS, Callaway CW, Carson AP, et al. American Heart Association Council on Epidemiology and Prevention Statistics Committee and Stroke Statistics Subcommittee. Heart Disease and Stroke Statistics-2019 Update: A Report From the American Heart Association. *Circulation*. 2019; 139: e56–e528. [Medline] [CrossRef]
- Banerjee S, Williamson D, Habib N, Gordon M, Chataway J. Human stem cell therapy in ischaemic stroke: a review. *Age Ageing*. 2011; 40: 7–13. [Medline] [CrossRef]
- Khanevski AN, Bjerkeim AT, Novotny V, Naess H, Thomassen L, Logallo N, et al. NOR-STROKE study group. Recurrent ischemic stroke: Incidence, predictors, and impact on mortality. *Acta Neurol Scand*. 2019; 140: 3–8. [Medline] [CrossRef]
- Yin P, Wei Y, Wang X, Zhu M, Feng J. Roles of Specialized Pro-Resolving Lipid Mediators in Cerebral Ischemia Reperfusion Injury. *Front Neurol*. 2018; 9: 617. [Medline] [CrossRef]
- Hu Y, Deng H, Xu S, Zhang J. MicroRNAs Regulate Mitochondrial Function in Cerebral Ischemia-Reperfusion Injury. *Int J Mol Sci*. 2015; 16: 24895–24917. [Medline] [CrossRef]
- Forouzanfar F, Shojapour M, Asgharzade S, Amini E. Causes and Consequences of MicroRNA Dysregulation Following Cerebral Ischemia-Reperfusion Injury. *CNS Neurol Disord Drug Targets*. 2019; 18: 212–221. [Medline] [CrossRef]
- Li P, Shen M, Gao F, Wu J, Zhang J, Teng F, et al. An Antagomir to MicroRNA-106b-5p Ameliorates Cerebral Ischemia and Reperfusion Injury in Rats Via Inhibiting Apoptosis and Oxidative Stress. *Mol Neurobiol*. 2017; 54: 2901–2921. [Medline] [CrossRef]
- Han XR, Wen X, Wang YJ, Wang S, Shen M, Zhang ZF, et al. Protective effects of microRNA-431 against cerebral ischemia-reperfusion injury in rats by targeting the Rho/Rho-kinase signaling pathway. *J Cell Physiol*. 2018; 233: 5895–5907. [Medline] [CrossRef]
- Kim T, Mehta SL, Morris-Blanco KC, Chokkalla AK, Chelluboina B, Lopez M, et al. The microRNA miR-7a-5p ameliorates ischemic brain damage by repressing α -synuclein. *Sci Signal*. 2018; 11: eaat4285. [Medline] [CrossRef]
- Liu FJ, Lim KY, Kaur P, Sepramaniam S, Armugam A, Wong PT, et al. microRNAs Involved in Regulating Spontaneous Recovery in Embolic Stroke Model. *PLoS One*. 2013; 8: e66393. [Medline] [CrossRef]
- Zhang SB, Liu TJ, Pu GH, Li BY, Gao XZ, Han XL. MicroRNA-374 Exerts Protective Effects by Inhibiting SP1 Through Activating the PI3K/Akt Pathway in Rat Models of Myocardial Ischemia-Reperfusion After Sevoflurane Preconditioning. *Cell Physiol Biochem*. 2018; 46: 1455–1470. [Medline] [CrossRef]
- Zhao Z, Zhao Y, Ying-Chun L, Zhao L, Zhang W, Yang JG. Protective role of microRNA-374 against myocardial ischemia-reperfusion injury in mice following thoracic epidural anesthesia by downregulating dystrobrevin alpha-mediated Notch1 axis. *J Cell Physiol*. 2019; 234: 10726–10740. [Medline] [CrossRef]
- van Amerongen R, Mikels A, Nusse R. Alternative wnt signaling is initiated by distinct receptors. *Sci Signal*. 2008; 1: re9. [Medline] [CrossRef]
- Kikuchi A, Yamamoto H, Sato A, Matsumoto S. Wnt5a: its signalling, functions and implication in diseases. *Acta Physiol (Oxf)*. 2012; 204: 17–33. [Medline] [CrossRef]
- Matsumoto S, Fumoto K, Okamoto T, Kaibuchi K, Kikuchi A. Binding of APC and dishevelled mediates Wnt5a-regulated focal adhesion dynamics in migrating cells. *EMBO J*. 2010; 29: 1192–1204. [Medline] [CrossRef]
- Yamamoto H, Kitadai Y, Yamamoto H, Oue N, Ohdan H, Yasui W, et al. Laminin gamma2 mediates Wnt5a-induced invasion of gastric cancer cells. *Gastroenterology*. 2009; 137: 242–252, 252.e1–252.e6. [Medline] [CrossRef]
- Nemeth MJ, Topol L, Anderson SM, Yang Y, Bodine DM. Wnt5a inhibits canonical Wnt signaling in hematopoietic stem cells and enhances repopulation. *Proc Natl Acad Sci USA*. 2007; 104: 15436–15441. [Medline] [CrossRef]
- Kumawat K, Gosens R. WNT-5A: signaling and functions in health and disease. *Cell Mol Life Sci*. 2016; 73: 567–587. [Medline] [CrossRef]
- McDonald SL, Silver A. The opposing roles of Wnt-5a in cancer. *Br J Cancer*. 2009; 101: 209–214. [Medline] [CrossRef]
- Blumenthal A, Ehlers S, Lauber J, Buer J, Lange C, Goldmann T, et al. The Wingless homolog WNT5A and its receptor Frizzled-5 regulate inflammatory responses of human mononuclear cells induced by microbial stimulation. *Blood*. 2006; 108: 965–973. [Medline] [CrossRef]
- Ouchi N, Higuchi A, Ohashi K, Oshima Y, Gokce N, Shibata R, et al. Sfrp5 is an anti-inflammatory adipokine that modulates metabolic dysfunction in obesity. *Science*. 2010; 329: 454–457. [Medline] [CrossRef]
- Nakamura K, Sano S, Fuster JJ, Kikuchi R, Shimizu I, Ohshima K, et al. Secreted Frizzled-related Protein 5 Diminishes Cardiac Inflammation and Protects the Heart from Ischemia/Reperfusion Injury. *J Biol Chem*. 2016; 291: 2566–2575. [Medline] [CrossRef]
- Wei X, Gong J, Ma J, Zhang T, Li Y, Lan T, et al. Targeting the Dvl-1/ β -arrestin2/JNK3 interaction disrupts Wnt5a-JNK3 signaling and protects hippocampal CA1 neurons during cerebral ischemia reperfusion. *Neuropharmacology*. 2018; 135: 11–21. [Medline] [CrossRef]
- Chen J, Sanberg PR, Li Y, Wang L, Lu M, Willing AE, et al. Intravenous administration of human umbilical cord blood reduces behavioral deficits after stroke in rats. *Stroke*. 2001; 32: 2682–2688. [Medline] [CrossRef]
- Zhang W, Wang Y, Bi G. Limb remote ischaemic postconditioning-induced elevation of fibulin-5 confers neuroprotection to rats with cerebral ischaemia/reperfusion injury: Activation of the AKT pathway. *Clin Exp Pharmacol Physiol*. 2017; 44: 656–663. [Medline] [CrossRef]
- Halleskog C, Dijksterhuis JP, Kilander MB, Becerril-Ortega J, Villacusa JC, Lindgren E, et al. Heterotrimeric G protein-dependent WNT-5A signaling to ERK1/2 mediates distinct aspects of microglia proinflammatory transformation. *J Neuroinflammation*. 2012; 9: 111. [Medline] [CrossRef]
- Ding S, Xu Z, Yang J, Liu L, Huang X, Wang X, et al. The Involvement of the Decrease of Astrocytic Wnt5a in the Cognitive Decline in Minimal Hepatic Encephalopathy. *Mol Neurobiol*. 2017; 54: 7949–7963. [Medline] [CrossRef]
- Peña ID, Borlongan C, Shen G, Davis W. Strategies to Extend Thrombolytic Time Window for Ischemic Stroke Treatment: An Unmet Clinical Need. *J Stroke*. 2017; 19: 50–60. [Medline] [CrossRef]
- Datta A, Sarmah D, Mounica L, Kaur H, Kesharwani R, Verma G, et al. Cell Death Pathways in Ischemic Stroke and Targeted Pharmacotherapy. *Transl Stroke Res*. 2020; 11: 1185–1202. [Medline] [CrossRef]
- Yaghi S, Willey JZ, Cucchiara B, Goldstein JN, Gonzales NR, Khatri P, et al. American Heart Association Stroke Council; Council on Cardiovascular and Stroke Nursing; Council on Clinical Cardiology; and Council on Quality of Care and Outcomes Research. Treatment and Outcome of Hemorrhagic

- Transformation After Intravenous Alteplase in Acute Ischemic Stroke: A Scientific Statement for Healthcare Professionals From the American Heart Association/American Stroke Association. *Stroke*. 2017; 48: e343–e361. [[Medline](#)] [[CrossRef](#)]
31. Patel RAG, McMullen PW. Neuroprotection in the Treatment of Acute Ischemic Stroke. *Prog Cardiovasc Dis*. 2017; 59: 542–548. [[Medline](#)] [[CrossRef](#)]
 32. Venkat P, Shen Y, Chopp M, Chen J. Cell-based and pharmacological neurorestorative therapies for ischemic stroke. *Neuropharmacology*. 2018; 134:(Pt B): 310–322. [[Medline](#)] [[CrossRef](#)]
 33. He CW, Liao CP, Pan CL. Wnt signalling in the development of axon, dendrites and synapses. *Open Biol*. 2018; 8: 8. [[Medline](#)] [[CrossRef](#)]
 34. McLeod F, Salinas PC. Wnt proteins as modulators of synaptic plasticity. *Curr Opin Neurobiol*. 2018; 53: 90–95. [[Medline](#)] [[CrossRef](#)]
 35. Li K, Ding D, Zhang M. Neuroprotection of Osthole against Cerebral Ischemia/Reperfusion Injury through an Anti-apoptotic Pathway in Rats. *Biol Pharm Bull*. 2016; 39: 336–342. [[Medline](#)] [[CrossRef](#)]
 36. Jung YS, Oh AY, Park HP, Hwang JW, Lim YJ, Jeon YT. Post-ischemic administration of pravastatin reduces neuronal injury by inhibiting Bax protein expression after transient forebrain ischemia in rats. *Neurosci Lett*. 2015; 594: 87–92. [[Medline](#)] [[CrossRef](#)]
 37. Jiang R, Liao J, Yang MC, Deng J, Hu YX, Li P, et al. Lidocaine mediates the progression of cerebral ischemia/reperfusion injury in rats via inhibiting the activation of NF- κ B p65 and p38 MAPK. *Ann Transl Med*. 2020; 8: 548. [[Medline](#)] [[CrossRef](#)]
 38. Puig B, Brenna S, Magnus T. Molecular Communication of a Dying Neuron in Stroke. *Int J Mol Sci*. 2018; 19: 19. [[Medline](#)] [[CrossRef](#)]
 39. Zhang P, Yang L, He H, Deng Y. Differential variations of autophagy and apoptosis in permanent focal cerebral ischaemia rat model. *Brain Inj*. 2017; 31: 1151–1158. [[Medline](#)] [[CrossRef](#)]